QUANTUM GASES

Pauli blocking of light scattering in degenerate fermions

Yair Margalit[1,2]*, Yu-Kun Lu[1,2], Furkan Çağrı Top[1,2], Wolfgang Ketterle[1,2]

Pauli blocking of spontaneous emission is responsible for the stability of atoms. Electrons cannot decay to lower-lying internal states that are already occupied. Pauli blocking also occurs when free atoms scatter light elastically (Rayleigh scattering) and the final external momentum states are already populated. This was predicted more than 30 years ago but is challenging to realize experimentally. Here, we report on Pauli blocking of light scattering in a dense quantum-degenerate Fermi gas of ultracold lithium atoms. When the Fermi momentum is larger than the photon recoil, most final momentum states are within the Fermi surface. At low temperature, we find that light scattered even at large angles is suppressed by 37% compared with higher temperatures, where atoms scatter at the single-atom Rayleigh scattering rate.

Suppression of light scattering in ultracold Fermi gases has been predicted in works dating back to 1990 (*1*–*8*). The basic phenomenon is shown in Fig. 1. Light scattering between photon states with wave vectors k_i and k_f transfers momentum $\hbar q = \hbar(k_i - k_f) = 2\hbar k \sin\theta/2$, where $\hbar k_i$ is the initial photon momentum, $\hbar k_f$ is the final photon momentum, and θ is the scattering angle. When the Fermi momentum $\hbar k_F$ of a zero-temperature Fermi gas is larger than the momentum transfer $\hbar q$, light scattering is strongly suppressed and can occur only near the Fermi surface, whereas for temperatures $T \geq T_F$, the scattering rate per atom approaches the independent atom limit. This smooth transition versus temperature has been theoretically studied, including by averaging over the inhomogeneous density distribution of a harmonically trapped atom cloud (*6*).

Experiments on ultracold atoms have deepened our understanding of basic physical phenomena by realizing paradigmatic idealized situations where the phenomenon is observed in its most direct and transparent form. These realizations then become building blocks for more-complex systems. Examples include the realization of Bose-Einstein condensation (BEC), the BEC–Bardeen-Cooper-Schrieffer (BCS) crossover in fermions, band structure phenomena of noninteracting atoms in optical lattices, and Mott insulators in optical lattices (*9*). Here, we study, in a highly idealized situation, how ultracold fermions scatter light and observe the suppression of light scattering caused by Pauli blocking in a degenerate Fermi gas. Recently, we have been able to prepare ultracold fermions at very high densities (up to $n = 3 \times 10^{15}$ cm^{-3}) (*10*), where the Fermi energy is 50 times as high as that of the photon recoil energy $\hbar^2 k_i^2/2m$ of 73.9 kHz (where m is the lithium atomic mass). Using this sample, we have now performed light-scattering experiments in the simplest possible limit, at detunings Δ from the atomic resonance of more than 100 GHz, or 17,000 linewidths Γ. Therefore, despite high atomic densities $n \approx 1.2/\lambda\!\!\!^{-3}$ and high resonant optical densities $6\pi n \lambda\!\!\!^{-2} l \approx 44{,}000$ (where $\lambda\!\!\!^{-} = 1/k$ and l is the length of the atom cloud), we realize the limit where both the absorptive and dispersive parts of the index of refraction are negligible. In general, optical properties become complicated in the regime of high densities thanks to strong Lorentz-Lorentz corrections (*11*) and dipolar interactions between the atoms (*12*). These corrections are often expanded in the parameter $n\alpha$, where α is the atomic polarizability, given for a two-level atom by $\alpha = 6\pi\lambda\!\!\!^{-3}\Gamma/(\Delta + i\Gamma)$. At our detunings, the parameter $n\alpha \approx 1/800$, and those corrections are negligible. Also, at detunings larger than the fine-structure splitting of 10 GHz, optical pumping to other hyperfine states is suppressed. At 100-GHz detuning, the branching ratio is <1% for any polarization of light, so no special cycling transition is needed. We use rather weak and long laser pulses with a Rayleigh scattering rate around or below 1 photon per atom during 1 ms to stay far away from nonlinear collective light scattering (*13*).

Ultracold lithium clouds were prepared as in our previous work (*10*). In short, ^{23}Na and ^{6}Li atoms are first laser cooled and then transferred into a quadrupole magnetic trap with an optical plug (*14*). Forced microwave evaporation of the Na atoms (*15*) sympathetically cools the lithium atoms. The lithium atoms are transferred into a single-beam 1064-nm optical dipole trap with variable spot size and power, which controls the trap volume and densities. A partially nonadiabatic radio-frequency (RF) Landau-Zener sweep transfers the majority of the atoms to the collisionally stable lowest Zeeman state $|F = 1/2, m_F = 1/2\rangle \equiv |1\rangle$ while keeping ~7% in the original state $|3/2, 3/2\rangle \equiv |6\rangle$. This creates a spin mixture with s-wave interactions, which allows for efficient evaporative cooling into quantum degeneracy. Decreasing the spot size of the trapping beam creates a tighter trap with frequencies of $\omega_r/2\pi$ = 34 kHz and $\omega_z/2\pi$ = 770 kHz in the radial and axial directions, respectively. The atoms are exposed to a final stage of evaporative cooling by tilting the trapping potential with a magnetic gradient for 1.5 s. A typical sample contains $N \simeq 8 \times 10^5$ ^{6}Li atoms at $T/T_F \simeq 0.2$, with a Fermi temperature of $T_F = \hbar(\omega_r^2 \omega_z 6N)^{1/3} = 70$ μK. This corresponds to a density of ~1×10^{15} cm^{-3} and an on-resonance optical density of ~25,000. We can produce even higher densities of up to 3×10^{15} cm^{-3} and Fermi energies of 190 μK, but they suffer from three-body losses and associated heating [which occur even in a spin-polarized sample (*10*)]. As the final step before the light-scattering experiment, the majority of the atoms are transferred by the same RF Landau-Zener sweep back to state 6, leaving ≤10% of

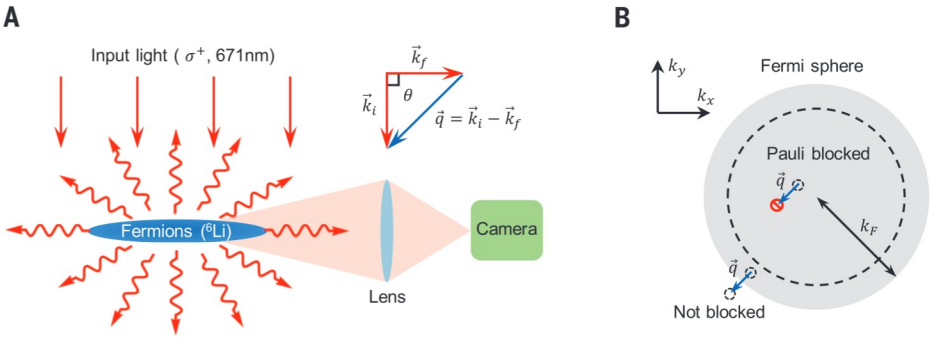

Fig. 1. Schematic of the experiment. (**A**) Degenerate fermionic lithium atoms are confined in an optical dipole trap and illuminated with a laser beam. Scattered photons impart momentum transfers of $\hbar q$ to the atoms and are detected at a scattering angle of 90°. (**B**) Mechanism of Pauli blocking in degenerate Fermi gases. At temperature T = 0, the atoms occupy a Fermi sphere in momentum space with radius $\hbar k_F$. For $q \ll k_F$, atoms can scatter light only from the outer shell of the Fermi sphere (of width $\hbar q$), where they can reach an unoccupied final momentum state. No scattering is possible for atoms within the dashed circle.

[1]Research Laboratory of Electronics, MIT-Harvard Center for Ultracold Atoms, Massachusetts Institute of Technology, Cambridge, MA 02139, USA. [2]Department of Physics, Massachusetts Institute of Technology, Cambridge, MA 02139, USA.
*Corresponding author. Email: margalya@mit.edu

the total number in state 1 to ensure thermalization. State 6 has a cycling transition that matters only at smaller detunings. The number of atoms in the trap is measured using standard time-of-flight absorption imaging with an estimated uncertainty of up to 40%.

After cooling to the lowest temperature, the sample is heated either by strongly modulating the trapping potential or by the scattering of light. For the observation of suppressed light scattering, we typically scatter 0.4 photons per atom during 25 ms and collect the fluorescence at a right angle with an imaging system with a collection efficiency of 0.31% (calibrated by on-resonant light scattering of a laser beam with known power and beam waist). This scattering corresponds to a recoil heating of ~4.6% of the original temperature. Given that we have reached quantum degeneracy far above the recoil temperature, scattering even a few photons does not cause substantial heating. The size of the laser beam is chosen to be much larger than the cloud size (14 times as large axially and 33 times as large radially) so that the intensity inhomogeneity across the atom cloud is negligible (*13*).

Figure 2 shows the main result of this paper—the suppression of light scattering by a degenerate Fermi gas. For each shot, the number of scattered photons is recorded, and the number of atoms and the temperature are obtained by time-of-flight absorption imaging. Thus, we measure the number of scattered photons per atom as a function of the cloud's temperature, and we observe that, in the degenerate regime ($T/T_F \approx 0.2$), the atoms scatter ~35% less light thanks to Pauli blocking compared with the unblocked case. Results are limited to $T/T_F \leq 0.8$ to reduce systematic errors, such as atom loss by spilling caused by the finite trap depth. Our observations are in good agreement with theoretical calculations for a trapped cloud of atoms (*6*). The theoretical model extends the treatment of (*6*) to the Gaussian potential of the optical dipole trap (*13*). Compared with a harmonic trap, the anharmonicites lead to smaller Pauli blocking (for our ratio of trap depth to E_F of ≈5.7), and the light-scattering rate approaches the nondegenerate limit to within 2% at $T/T_F = 0.7$. The lowest temperatures are measured from the shape of the degenerate cloud [by fitting to a polylog function (*16*)], directly providing the fugacity or T/T_F without any correction parameters. For higher temperatures, when the cloud shape becomes Gaussian, this direct method fails, and we instead determine the temperature from Gaussian fits to the wings of the cloud and $k_B T_F = \hbar\left(\omega_r^2 \omega_z 6N\right)^{1/3}$ from the number count N, where k_B is the Boltzmann constant. For a broad range of intermediate temperatures, the two methods agree to within a correction factor that accounts for experimental drifts between the data run and when the N count and trap frequencies were carefully calibrated. This correction factor for Fermi energies (which varied for different data runs between 1.1 and 1.2) affects only the horizontal scale and not the Pauli suppression. For the comparison of experimental data with the theoretical curve in Fig. 2, the only adjustable parameter is the normalization of the high-temperature photon signal to 1. This normalization is equivalent to a calibration of the excitation and detection efficiencies for the exact experimental conditions in which the data were taken.

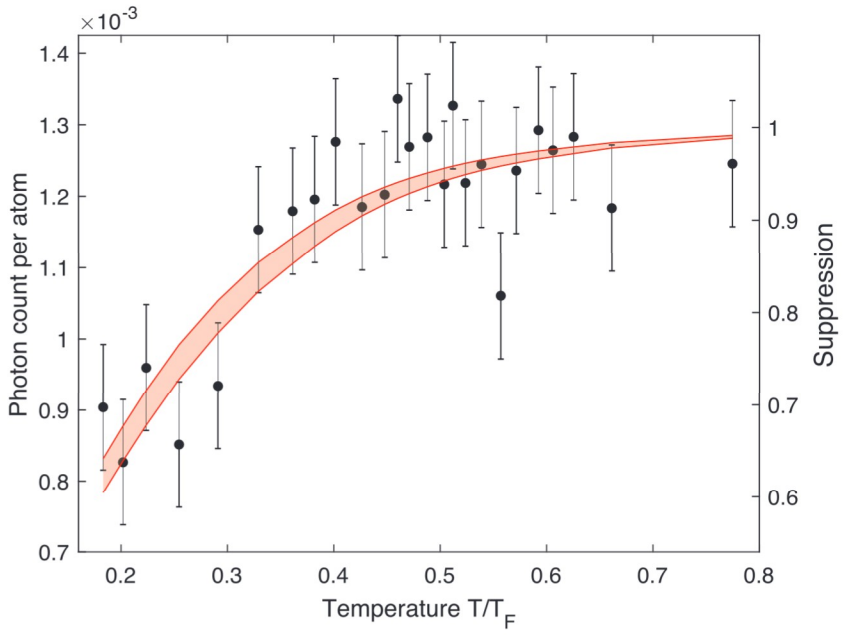

Fig. 2. Pauli blocking of light scattering. Photon count per atom as a function of the cloud's temperature, observed at a scattering angle of 90°. At a low temperature, the scattered light is reduced by 35% with respect to the unblocked case. The cloud is heated by turning the optical dipole trap off and on for a variable duration. The probe light is pulsed on for 25 ms at an intensity of 7.0×10^2 m W cm^{-2} and is detuned 100 GHz below the atomic resonance (located at 671 nm). The two solid red lines (enclosing the red-shaded region) show the theoretical prediction of the Pauli suppression factor (right *y* axis) for the optical dipole trap potential (see the text). The difference between the solid lines represents the uncertainty in the number of atoms (40%). There are no free-fitting parameters apart from the overall vertical scale relative to the data. The error bars in all of the figures are purely statistical and reflect one standard error of the mean. Data points here are each averaged over 12 samples. The constant error bars shown are averaged over the whole dataset and reflect the best estimate for the statistical uncertainty. The uncertainties are dominated by camera-read noise for the 81 pixels within the region of interest and fluctuations of light from the trapping laser, which propagates into the camera and could not be completely suppressed by filters.

Because light scattering heats up the cloud by photon recoil heating, Pauli suppression can be observed only for sufficiently short or weak laser pulses. This is demonstrated in Fig. 3, where we study the number of photons scattered per atom as a function of probe laser power for initially degenerate and nondegenerate clouds. For a nondegenerate cloud ($T/T_F \approx 0.7$), the photon scattering signal is linear in laser power for the whole range of powers studied, with a slope of 2.3 ± 0.09 [1/W] (Fig. 3B). For a degenerate cloud, there is an initial linear regime for low power (which was used for Fig. 2), but after scattering several photons per atom, the temperature increases owing to recoil heating, and the slope increases as a consequence of the gradual elimination of Pauli blocking. The blue line in Fig. 3A is a linear fit for the low-power part of the data (where Pauli blocking is present) and returns a slope of 1.7 ± 0.17 [1/W].

The larger cloud size in Fig. 3B and the use of a small probe beam effectively reduce the average light intensity by 18% compared with the result shown in Fig. 3A [evaluated using a simple parameter-free model that accounts for thermal expansion (*13*)]. After correcting for this, the ratio of the slopes at low and high temperature is 0.63 ± 0.07 and agrees within its uncertainty to the Pauli suppression factor of 0.65 in Fig. 2. We have observed similar behavior for widely different parameters of the atom cloud and the probe beam. However, we find that this way of characterizing Pauli blocking is less direct (as the cloud changes

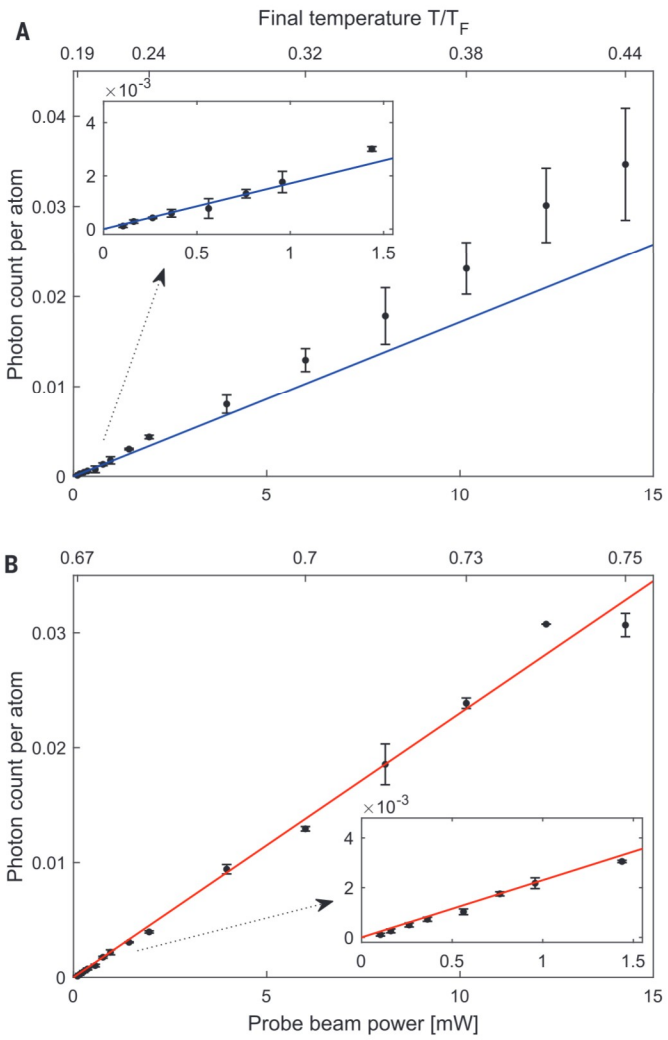

Fig. 3. Light scattering as a function of probe beam power. (**A** and **B**) We observe different slopes for low temperature, where Pauli blocking is present (A), and at high temperature (B). Solid lines are linear fits to the data [fit to the low-power part in (A) and to the full range in (B)]. The data in (B) were taken under similar experimental conditions as those in (A), but atoms were preheated to an initial temperature of T/T_F = 0.67. At these temperatures, the blocking effect should be only ~5%. For the degenerate cloud, the signal is linear only for small laser power thanks to recoil heating. The top *x* axis shows the final temperature (T/T_F), measured after releasing atoms from the trap. Detuning of the probe beam is $\Delta = -112$ GHz. Insets shows enlarged versions of the low-power region.

temperature during the probing) and more sensitive to fluctuations in the experiment than the method used for Fig. 2.

Because light scattering involves a (virtual) excited state, fermionic suppression of light scattering is related to Pauli suppression of spontaneous emission from an excited state embedded in a Fermi sea. The distinction between light scattering and spontaneous emission becomes important for an interacting system. It was shown theoretically that spontaneous emission in a zero-temperature Bose-Einstein condensate is enhanced by bosonic stimulation through the quantum depletion, whereas light scattering from a Bose-Einstein condensate is suppressed because the static structure factor $S(q) < 1$ owing to the phonon-dispersion relation (*17*).

So far, we have described Pauli blocking as a single-particle effect caused by Fermi statistics. However, because Fermi statistics create correlations between particles, one can also express Pauli blocking in terms of a pair correlation function. This will allow us to compare the suppression in our light-scattering experiment with other studies demonstrating fermionic suppression. The cross section of light (and also particle) scattering with momentum transfer $\hbar q$, $d\sigma/d\Omega$ is given by $S(q)$ times the single particle cross section $\sigma_0(q)$: $d\sigma/d\Omega = N\sigma_0(q)S(q)$ with N representing the number of fermions. $S(q)$ is given by the Fourier transform of the density-density correlation function. A homogeneous system with $S(q) = 0$ would not scatter light. Uncorrelated classical particles show Poissonian fluctuations implying $S(q) = 1$. Suppression of light scattering off fermions is caused by suppressed density fluctuations, implying $S(q) < 1$. Suppression of density fluctuations in cold fermion clouds has been directly observed in previous studies (*18*–*20*), where the atomic density was shown to have sub-Poissonian fluctuations. This immediately implies reduced light scattering at small angles of order k_F/k_i. We have now extended this work by suppressing light scattering at all angles and directly detecting the scattered photons at a large angle. In the absence of longer-range correlations, the density-density correlation function is expressed by the pair correlation function $g(r)$, which is the normalized probability of detecting two particles at separation r, so the structure factor can be written as (*21*)

$$S(q) = 1 + n\int d^3r[g(r) - 1]e^{-iq\cdot r} \qquad (1)$$

For a nondegenerate quantum gas, $g(r) - 1 \neq 0$ for $r < \Lambda_t$, where Λ_t is the thermal de Broglie wavelength (*22*)

$$g(r) \approx 1 \pm \exp\left(-2\pi r^2/\Lambda_t^2\right) \qquad (2)$$

resulting in

$$S(q) \approx 1 \pm D\exp\left(-q^2\Lambda_t^2/8\pi\right)/2^{3/2} \qquad (3)$$

where $D = n\Lambda_t^3$ is the peak phase space density reached around zero momentum. The averaged phase space density is $D/2^{3/2}$. The ± sign refers to bosons and fermions, respectively. The term "1" is the (normalized) contribution of the scattering of single atoms, whereas the second term is a consequence of nonvanishing interference terms involving light scattering by pairs of particles. Equation 3 can be generalized for degenerate gases (*22*) with the result that for fermions at zero temperature $S(q \to 0) = 0$, pair scattering completely cancels the scattering from single particles at angles for which $q \ll k_F$. This description emphasizes the central role of the pair correlations in the enhancement or suppression of light scattering. The pair correlation function has been directly observed in the suppression of elastic scattering (*23*) and inelastic scattering, including three-body recombination (*10*, *24*), which was crucial for the study of the BEC-BCS crossover (*25*), and the absence of interaction shifts in RF spectroscopy (*26*). We discuss in the supplementary materials (*13*) how the detuning dependence of inelastic light scattering can be used to map out the pair correlation function. Sometimes, these processes are described by Pauli suppression in the input channel (which is the p-wave), whereas the suppression of light scattering is regarded as Pauli suppression in the output channel. This distinction is correct, but it obscures the common origin of both effects, which are the pair correlations. Equation 1 is very general and applies also to colloidal particles with spatial correlations caused by interactions (*27*). It is only for noninteracting gases that quantum degeneracy is necessary to strongly modify the structure factor, and pair correlations have a one-to-one relation to bosonic enhancement or fermionic suppression.

We have directly observed Pauli blocking of light scattering. For our high densities, Pauli blocking is mainly limited by temperature, which can be lowered by an improved evaporation strategy addressing p-wave three-body recombination as the dominant loss mechanism (*10*). Pauli suppression can be used in

quantum simulations to create fermionic samples that are less sensitive to heating when probed or manipulated by laser light. There are still many unresolved questions in how dense atomic samples scatter light, involving dipole-dipole interactions and superradiant scattering (*12*), and fermionic clouds with reduced incoherent scattering are a promising system for further studies.

REFERENCES AND NOTES

1. K. Helmerson, M. Xiao, D. Pritchard, in *International Quantum Electronics Conference*, A. Owyoung, C. Shank, S. Chu, E. Ippen, Eds., vol. 8 of *OSA Technical Digest* (Optical Society of America, 1990).
2. J. Javanainen, J. Ruostekoski, *Phys. Rev. A* **52**, 3033–3046 (1995).
3. T. Busch, J. R. Anglin, J. I. Cirac, P. Zoller, *Europhys. Lett.* **44**, 1–6 (1998).
4. B. DeMarco, D. S. Jin, *Phys. Rev. A* **58**, R4267–R4270 (1998).
5. J. Ruostekoski, J. Javanainen, *Phys. Rev. Lett.* **82**, 4741–4744 (1999).
6. B. Shuve, J. H. Thywissen, *J. Phys. B At. Mol. Opt. Phys.* **43**, 015301 (2009).
7. B. O'Sullivan, T. Busch, *Phys. Rev. A* **79**, 033602 (2009).
8. R. M. Sandner, M. Müller, A. J. Daley, P. Zoller, *Phys. Rev. A* **84**, 043825 (2011).
9. I. Bloch, J. Dalibard, W. Zwerger, *Rev. Mod. Phys.* **80**, 885–964 (2008).
10. F. Ç. Top, Y. Margalit, W. Ketterle, *Phys. Rev. A* **104**, 043311 (2021).
11. J. D. Jackson, *Classical Electrodynamics* (Wiley, 1999).
12. B. Zhu, J. Cooper, J. Ye, A. M. Rey, *Phys. Rev. A* **94**, 023612 (2016).
13. Materials and methods are available as supplementary materials online.
14. K. B. Davis *et al.*, *Phys. Rev. Lett.* **75**, 3969–3973 (1995).
15. Z. Hadzibabic *et al.*, *Phys. Rev. Lett.* **91**, 160401 (2003).
16. W. Ketterle, M. W. Zwierlein, in *Ultracold Fermi Gases, Proceedings of the International School of Physics "Enrico Fermi"*, M. Inguscio, W. Ketterle, C. Salomon, Eds. (IOS Press, 2008).
17. A. Görlitz, A. P. Chikkatur, W. Ketterle, *Phys. Rev. A* **63**, 041601 (2001).
18. C. Sanner *et al.*, *Phys. Rev. Lett.* **105**, 040402 (2010).
19. T. Müller *et al.*, *Phys. Rev. Lett.* **105**, 040401 (2010).
20. A. Omran *et al.*, *Phys. Rev. Lett.* **115**, 263001 (2015).
21. D. Chandler, *Introduction to Modern Statistical Mechanics* (Oxford Univ. Press, 1987).
22. J. Bosse, K. N. Pathak, G. S. Singh, *Phys. Rev. E* **84**, 042101 (2011).
23. B. DeMarco, J. L. Bohn, J. P. Burke, M. Holland, D. S. Jin, *Phys. Rev. Lett.* **82**, 4208–4211 (1999).
24. D. S. Petrov, C. Salomon, G. V. Shlyapnikov, *Phys. Rev. Lett.* **93**, 090404 (2004).
25. T. Bourdel *et al.*, *Phys. Rev. Lett.* **93**, 050401 (2004).
26. S. Gupta *et al.*, *Science* **300**, 1723–1726 (2003).
27. A. Parola, R. Piazza, V. Degiorgio, *J. Chem. Phys.* **141**, 124902 (2014).
28. Y. Margalit, Figures data for "Pauli blocking of light scattering in degenerate fermions" (arXiv:2103.06921), *Zenodo* (2021); https://doi.org/10.5281/zenodo.5523336.
29. Y. Margalit, margalya/pauli-blocking: Release, version 1.0, Zenodo (2021); https://doi.org/10.5281/zenodo.5523379.

ACKNOWLEDGMENTS

We thank H. Son for comments on the manuscript. **Funding:** This work was supported by the NSF through the Center for Ultracold Atoms and grant no. 1506369, ARO-MURI Non-Equilibrium Many-Body Dynamics (grant no. W911NF-14-1-0003), AFOSR-MURI Quantum Phases of Matter (grant no. FA9550-14-10035), the ONR (grant no. N00014-17-1-2253), and a Vannevar-Bush Faculty Fellowship. **Author contributions:** All authors contributed to the concepts of the experiment; Y.M. and F.Ç.T. developed the sample preparation; Y.M. and Y.-K.L. designed the light-scattering setup and took and analyzed the data; and Y.M., Y.-K.L., and W.K. wrote the paper. **Competing interests:** The authors declare no competing interests. **Data and materials availability:** Data and code are deposited on Zenodo (*28*, *29*).

SUPPLEMENTARY MATERIALS

science.org/doi/10.1126/science.abi6153
Materials and Methods
Figs. S1 to S4
References (*30*–*33*)

19 March 2021; accepted 4 October 2021
10.1126/science.abi6153

Science

Pauli blocking of light scattering in degenerate fermions

Yair MargalitYu-Kun LuFurkan Ça#r# TopWolfgang Ketterle

Science, 374 (6570), • DOI: 10.1126/science.abi6153

Photons not welcome

Two identical fermions cannot occupy the same quantum state, or so says the Pauli principle. For a cold gas of fermionic atoms, this means that all states up to the Fermi energy will be occupied, with only the atoms with the highest energy able to change their state. Such conditions have long been predicted to suppress light scattering off gases because the atoms receiving a kick from collisions with photons would have no state to move to. Deb *et al*., Margalit *et al*., and Sanner *et al*. now describe this so-called Pauli blocking of light scattering. —JS

Science (ISSN) is published by the American Association for the Advancement of Science. 1200 New York Avenue NW, Washington, DC 20005. The title *Science* is a registered trademark of AAAS.